Article

Moisture Origin and Transport for Extreme Precipitation over Indonesia's New Capital City, Nusantara in August 2021

Anis Purwaningsih [1,*], Sandro W. Lubis [1,2], Eddy Hermawan [1], Dita Fatria Andarini [1], Teguh Harjana [1], Dian Nur Ratri [3,4], Ainur Ridho [5], Risyanto [1] and Akas Pinaringan Sujalu [6]

1 Research Center for Climate and Atmosphere (PRIMA), National Research and Innovation Agency (BRIN), Jakarta 10340, Indonesia
2 Department of Mechanical Engineering, Rice University, 5100 Main Str., Houston, TX 77005, USA
3 Meteorological, Climatological, and Geophysical Agency, Jakarta 10720, Indonesia
4 Meteorology and Air Quality Group, Wageningen University and Research, Droevendaalsesteeg, 6708 Wageningen, The Netherlands
5 Cerdas Antisipasi Risiko Bencana Indonesia (CARI), Bandung 40293, Indonesia
6 Departement Agrotechnology, Faculty of Agriculture, Universitas 17 Agustus 1945, Samarinda 75123, Indonesia
* Correspondence: anis.purwaningsih@brin.go.id

Abstract: Nusantara, Indonesia's new capital city, experienced a rare extreme rainfall event on 27–28 August 2021. This heavy rainfall occurred in August, the driest month of the year based on the monthly climatology data, and caused severe flooding and landslides. To better understand the underlying mechanisms for such extreme precipitation events, we investigated the moisture sources and transport processes using the Lagrangian model HYSPLIT. Our findings revealed that moisture was mostly transported to Nusantara along three major routes: from Borneo Island (BRN, 53.73%), the Banda Sea and its surroundings (BSS, 32.03%), and Sulawesi Island (SUL, 9.05%). Overall, BRN and SUL were the main sources of terrestrial moisture, whereas the BSS was the main oceanic moisture source, having a lower contribution than its terrestrial counterpart. The terrestrial moisture transport from BRN was mainly driven by the large-scale high vortex flow, whereas the moisture transport from the SUL was driven by the circulation induced by boreal summer intraseasonal oscillation (BSISO) and low-frequency variability associated with La Niña. The near-surface oceanic moisture transport from BSS is primarily associated with prevailing winds due to the Australian monsoon system. These insights into moisture sources and pathways can potentially improve the accuracy of predictions of summer precipitation extremes in Indonesia's new capital city, Nusantara, and benefit natural resource managers in the region.

Keywords: moisture sources; moisture transport; extreme precipitation; Nusantara; Indonesia

1. Introduction

Indonesia's parliament has decided to move the national capital city from Jakarta to the province of East Kalimantan on the island of Borneo [1]. The name of this new capital city is Nusantara, commonly known as Ibu Kota Negara Baru in Bahasa (see Figure 1). This city is a part of several subdistricts in the Penajam Paser Utara regency and the Kutai Kartanegara regency in the province of East Kalimantan [2]. There are several reasons why the government is relocating the national capital city to Nusantara, such as population distribution, addressing the clean water source crisis on Java Island, and boosting economic growth outside of Java Island [3].

According to the Regional Disaster Management Agency, Nusantara has experienced several flood disasters over the past few years. According to documentation from January 2019 to January 2022, there have been 15 flooding events [4]. One of the major floods occurred on 27–28 August 2021 and strongly affected human lives and society [4]. The heavy

precipitation on those days was considered unusual because it lasted more than 11 h and occurred during the dry season [5]. During this period, the daily rainfall accumulation recorded by Sepaku Observational Station reached 82 mm/day, which was more than an extreme rainfall threshold based on statistical analysis. The lower limit of the 99th percentile of daily rainfall distribution is 64 mm/day. This recorded daily precipitation is ranked as the twentieth-highest daily rainfall over 45 cases of precipitation, exceeding the extreme rainfall threshold over this location. The extreme rainfall subsequently triggered floods and landslides in several places in East Kalimantan. Investigating the underlying physical process of this extreme event can improve our understanding of the driving mechanisms of unusual extreme rainfall events during the dry season in Indonesia's new capital city, Nusantara, and potentially improve the prediction of summer rainfall over the region.
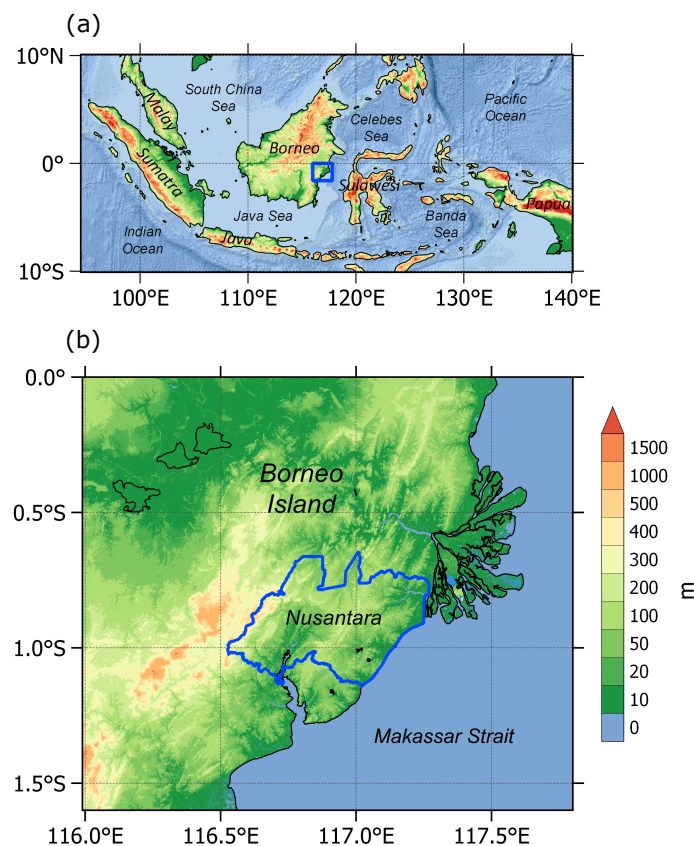

Figure 1. Topography map of (**a**) the study area (blue rectangle) located in the middle of the Maritime Continent on the eastern Borneo Island (**b**) the administrative borderline of Nusantara (blue looped-line).

There is still a lack of understanding of the mechanisms causing the extreme rainfall over Nusantara in the province of East Kalimantan. This is likely due to the complexity of the dynamics of the atmosphere over the region, which is located over the equator. In general, the precipitation in East Kalimantan has a typical monsoonal-type pattern [6]. This monsoonal type is characterized by a cycle of months with lower and higher rainfall intensities during the year, with the driest months from June to August and the wettest months from December to February [6]. Observational data from the Indonesian Agency for Meteorological Climatological and Geophysics (BMKG) weather station over Sepaku, East Kalimantan, verify data on the driest and wettest months in this area. The climatology of monthly rainfall indicates that August is the driest month of the year, with a monthly mean rainfall intensity of 56 mm/month. The wettest month is in December, with a monthly rainfall intensity of 150 mm/month. In addition, the heavy rainfall over the

central Maritime Continent is also often associated with an organized convective system associated with boreal summer intraseasonal oscillation (BSISO) [7,8]. BSISO is a large-scale weather system that strongly influences intraseasonal rainfall variability during boreal summer as a result of the interaction between the Madden Julian Oscillation (MJO) and the monsoonal system [7–9]. Furthermore, the tropical synoptic activities associated with tropical highs and lows in a range of approximately 2–8 days also often play a key role in modulating the summertime convection that causes day-to-day weather variations and heavy rainfall over East Kalimantan during boreal summer [10]. In addition, the rainfall variation in East Kalimantan is also affected by the interannual variability of the tropical sea surface temperature (SST) in the Pacific and Indian Oceans associated with El Niño Southern Oscillation (ENSO) [11,12]. In particular, El Niño causes a prolonged dry season, whereas La Niña is related to high rainfall above the average [13]. Moreover, the modulation of rainfall over the maritime continent is also influenced by the Inter-tropical Convergence Zone (ITCZ) [14,15] and its interaction with other atmospheric phenomena, such as ENSO [16,17]. All these atmospheric drivers acting on different timescales can modulate and influence the formation and development of extreme summertime rainfall events in Nusantara.

The occurrence of extreme rainfall events is associated with the high moisture content in the atmosphere [18]. How extreme the rainfall is depends on how long the condition of high moisture content over the region persists [19]. Previous studies have shown that moisture is one of the primary rainfall sources for the development of torrential rainfall events. For example, an investigation by Nie and Sun [20] u) using a Lagrangian approach concluded that the extreme precipitation event over Henan in July 2021 was driven by moisture from Southern China and the western North Pacific. In addition, Zhou et al. [21] studied water vapor transports associated with torrential rainfall from April to September from 2008 to 2015 over Xinjiang, China. They found that water vapor related to heavy precipitation events is mostly transported by westerly winds. Moreover, Tan et al. [22] analyzed a dominant contribution to the precipitation over western North America when the atmospheric river and extreme precipitation occurred simultaneously. They also found that moisture flux convergence is the key. The aforementioned studies suggest that it is important to evaluate the source of the moisture transport responsible for the precipitation extremes to better understand the underlying mechanisms of such events.

In this study, we investigate the sources of moisture and transport for the extreme precipitation events in Nusantara on 27–28 August 2021 that caused catastrophic flooding and significant socioeconomic effects in many places [23,24]. We employed a Hybrid Single-Particle Lagrangian Integrated Trajectory Model (HYSPLIT) to track the origin of the moisture and transports responsible for the extreme precipitation event. Furthermore, this study explores the underlying dynamics that drive such moisture transport during extreme rainfall events, similar to the previous studies [25,26]. This is the first comprehensive study that applies a Lagrangian moisture analysis to understand the cause of the extreme precipitation event in Indonesia. We anticipate that this study will provide knowledge about the source monitoring and prediction system for water vapor transport in East Kalimantan, especially over the new capital of Indonesia, Nusantara. It is also expected that our system can be a support tool for decision-makers to help users develop a hydrometeorological disaster risk reduction strategy. We hope that this research can be one of the integration and synchronization steps needed to understand the factors that cause flooding in the Nusantara area. Later, our findings are expected to be a consideration in environmental development planning to mitigate flooding natural disasters. In Section 2, we describe the data and methods. The results are presented in Section 3 before the article concludes with a discussion of the findings in Section 4.

2. Data and Methods

2.1. Precipitation Data and Reanalysis Data

The half-hourly gridded rainfall dataset produced by the Global Precipitation Measurement (GPM) Integrated Multi-satellite Retrievals for GPM (IMERG) with a $0.1° \times 0.1°$ spatial resolution was employed in this study to investigate the characteristics of heavy rainfall [27]. We used the rainfall data for the period of 27 August 2021 14Z to 28 August 2021 08Z from the IMERG version 3 final (IMERG-F), a final product of IMERG that was adjusted by the analysis of the monthly Global Precipitation Climatology Centre (GPCC) gauge [28]. These data were accessed from Goddard Earth Sciences Data and Information Services Center (https://disc.gsfc.nasa.gov/datasets/, accessed on 25 March 2022). Moreover, the hourly rainfall data from the Indonesian Agency for Meteorological Climatological and Geophysics (BMKG) weather station over Sepinggan, Balikpapan, was used for the same period.

This study also used the top brightness temperature (TBB) of the Himawari-8 satellite retrieved from the Himawari receiver at the National Research and Innovation Agency (BRIN), which has a spatial resolution of 4 km and a temporal resolution of 1 h. The infrared channel at 10.4 μm (Band 13) was applied to identify the evolution of the mesoscale convective system (MCS) associated with heavy precipitation. Generally, the Himawari-8 with an interval of 10 min for the full disk scans creates the possibility of monitoring more detailed clouds [29,30]. The MCS in the study were tracked by using the GTG (Grab 'em, Tag 'em, Graph 'em) algorithm [31], which has been applied in the previous study investigating the heavy rainfall events in some regions of Indonesia [25,30,32].

To analyze the moisture transport and contribution, this study utilized the European Center for Medium-Range Weather Forecast reanalysis 5 (ERA5) data, with a $0.25° \times 0.25°$ horizontal resolution and hourly temporal interval [33]. The ERA5 data on the single surface level and pressure levels for the period of 24 to 27 August 2021 were used to track the moisture source of heavy rainfall using the HYSPLIT and calculate the vertically integrated water vapor transport (IVT). In addition, we also used horizontal wind data and specific humidity at pressure levels for the same period to analyze the meteorological drivers during extreme precipitation.

2.2. HYSPLIT Model and Backward Trajectories

The Lagrangian approach using the HYSPLIT model, version 5.1, was applied to calculate the back trajectories of moisture properties that triggered the heavy precipitation over Nusantara during the flood event on 28 August 2021. The HYSPLIT model, as developed by NOAA's Air Resources Laboratory, is one of the most extensively used models for atmospheric transport and dispersion analyses [34,35]. In this study, we ran a total of 99 grid points at the heavy rainfall area and its surrounding area in Nusantara (116.2°–117.2° E and 0.8°–1.6° S) with a horizontal interval of 0.1° (Figure 2). The start time of each trajectory was set at the peak of heavy rainfall events (27 August 2021 at 18Z). Then, we calculated the 72 h backward trajectories within 11 different altitudes, from 500 m to 5500 m above the ground level (with intervals of 500 m), to analyze moisture transport and sources.
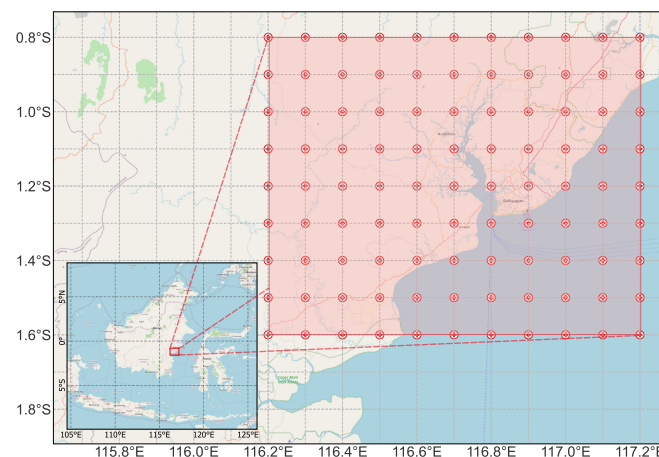
Figure 2. Release points of the moisture trajectories (from 116.2°–117.2° E and 0.8°–1.6° S, with an interval of 0.1°). The vertical resolution is 500 m, extending from 500 to 5500 m above the ground level (m agl).

2.3. Moisture Source Attribution

The contributions of different moisture sources that led to heavy precipitation in Nusantara were identified by applying the algorithm from Sodemann et al. [36]. We calculated the moisture changes of an air parcel during a time interval of 1 h using the following equation [37,38]:

$$\frac{Dq}{Dt} \approx \frac{\Delta q}{\Delta t} = E - P \left(gkg^{-1}h^{-1} \right) \tag{1}$$

$$\Delta q°(t) = q(\vec{x}(t)) - q(\vec{x}(t - 1h)) \tag{2}$$

Generally, the changes in specific humidity in a certain interval (Dq/Dt) show the net result of precipitation (P) and evaporation (E) processes along the trajectories [37]. A moisture source was identified through the trajectory locations (moisture intake event) if the moisture of a particle increases ($\Delta q° > 0$). Meanwhile, the precipitation was determined if the moisture decreases ($\Delta q° < 0$) [20,36]. To estimate the moisture source attribution of specific areas, we divided the region of the study area (11° S–9° N and 93°–133° E) into ten sub-regions by considering the land and ocean. Then, the 72 h evolution of moisture intake was calculated for each sub-region.

2.4. Clustering for the Trajectories

The backward trajectories simulated by the HYSPLIT model have two-dimensional locations (longitudes and latitudes) that can be categorized into several clusters. In this study, *k*-means clustering was performed to identify the main groups of trajectories. The *k*-means algorithm is an unsupervised clustering method that classifies given data into a set of *k* groups according to their characteristics [39,40]. This method also has the ability to produce more stable cluster boundaries [41]. In addition, to determine the best number of clusters, we applied the within-cluster sum of square errors (WCSS) metric based on the elbow method [15,41]. The optimum number is selected when the WCSS reaches the minimum value, which is 3 cluster centers in our study.

2.5. Atmospheric Mechanism Analysis

To analyze the possible mechanisms that modulate the pathways of moisture transport on extreme precipitation simulated by the HYSPLIT model, we calculated the daily vertically integrated water vapor transport (IVT) between 1000 hPa and 300 hPa. Then, stream functions of IVT were decomposed for different periods that represent the contribution of the atmospheric variability components using the bandpass filter method. This method al-

lows defining certain filter cutoff frequencies depending on the study analysis as it removes the low-frequency and high-frequency components [42]. In this study, we filtered the IVT stream function into the period of 10–20 days, 30–60 days, >120 days, and residual to analyze the dynamical process of high-frequency modes, BSISO, low-frequency oscillation, and other variabilities.

3. Results

3.1. Overview of the Extreme Precipitation Event

Figure 3a shows the precipitation accumulation distribution from 14Z on 27 August 2021 to 08Z on 28 August 2021. The figure indicates that intense precipitation occurred in eastern Borneo, central Borneo, southern Sulawesi, and the Banda Sea. It also shows that the coastal area of Nusantara experienced heavy rainfall (precipitation of more than 100 mm); however, inland, the intensity decreased. The bar chart in Figure 3 shows that the rainfall in Nusantara started at 14Z and reached its peak at 18Z, with a maximum intensity of 15 mm/h, decreasing thereafter. The total precipitation from 14Z on 27 August 2021 to 08Z 28 August 2021 was 80 mm, which reached the 99th percentile climatology value of the daily precipitation amount in this area; hence, it was categorized as an extreme rainfall event.

IVT between 1000 and 300 hPa (color shading) superimposed with streamlines of the vertically integrated moisture flux (contour lines) during the peak of precipitation at 18Z on 27 August 2021 is shown in Figure 3b. There was a flow of moisture transported westward along the surrounding area of the Banda Sea and the Flores Sea before its break into the Makassar Strait and the Java Sea. The moisture flux streamline shows a converged path pattern from the peripheral region into the middle of Borneo Island. In addition, it is evident that a vortex-like pattern was established on the sea west of Borneo, which is also a prominent feature associated with the flux during the extreme precipitation period. These results provide hints about possible sources of the moisture transport responsible for the extreme rainfall event in Nusantara during this period, which will be further discussed in Sections 3.1 and 3.2.

It is important to note that the occurrence of the rare extreme rainfall event on 27–28 August 2021 during the dry season in Nusantara was associated with the formation and development of the MCS. Figure 4 shows the three-hour evolution of the MCS from the Himawari-8 satellite superimposed with the rainfall rate from GPM IMERG for the period of 27 August at 12Z to 28 August 2021 at 9Z. These complex convective clouds were developed and lasted for about 22 h and were concentrated primarily on the central area of Borneo. The MCS initiated from several small cloud clusters emerged locally in the northern part of Nusantara (see Figure 4a). It grew constantly, becoming larger and mostly covering the central area of the island and a minor part of eastern Borneo, including Nusantara (see Figure 4b,c), which generated a peak rainfall rate of 18Z on 27 August. On the other side, another cloud cluster developed along the coast of east Borneo, starting at 18Z on 27 August 2021 and eventually merging to form the second MCS surrounding Nusantara three hours later (see Figure 4d). Afterward, the first MCS, which had previously developed in central Borneo, merged with the second MCS, which developed along the coast of east Borneo (see Figure 4e). Then they gradually dissipated, followed by the decreasing intensity of rainfall (see Figure 4f–h).

3.2. Moisture Sources and Transport for Summer Extreme Precipitation in Nusantara

One of the key factors that favor the occurrence of deep convection, such as an MCS, and extreme rainfall is the substantial moisture content in the lower atmosphere. Our results so far suggest that the moisture responsible for the formation of MCS and extreme rainfall events in Nusantara was transported from different regions (see Figures 3 and 4). Therefore, it is important to investigate where the atmospheric moisture came from that favored the MCS and consequently the extreme total amounts of precipitation in Nusantara (see Figure 3). In the following section, we will discuss in detail the origin, pathways, and contributions of moisture from different sources as well as the role of atmospheric

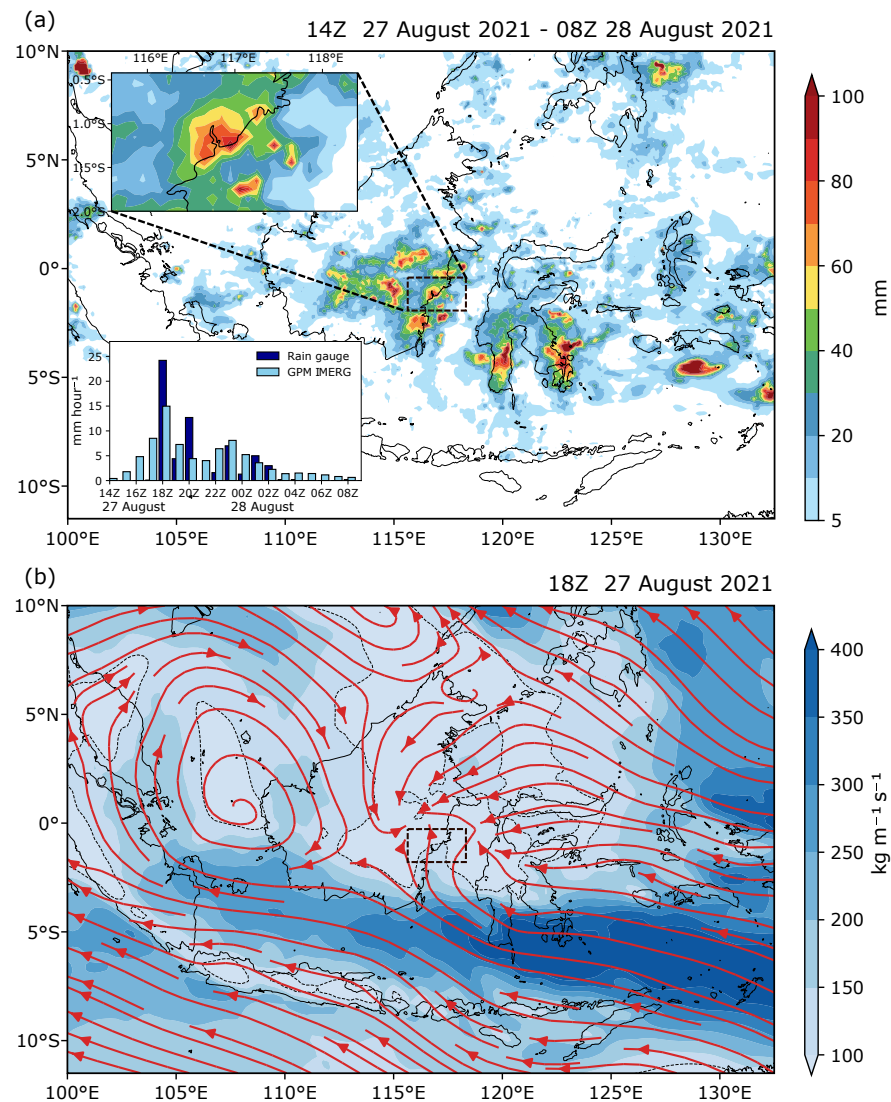modes in driving the moisture transport during extreme precipitation events in Nusantara on 27–28 August 2021.

Figure 3. (**a**) Spatial distribution of precipitation accumulation between 14Z 27 August 2021 to 08Z 28 August 2021 (color shading) in Indonesia. The inset map denotes the precipitation accumulation zoomed-in over the Nusantara city region. The time series histogram shows the hourly precipitation observed by rain gauge of Sepinggan (dark blue) and area-averaged hourly precipitation of Nusantara and the surrounding area based on GPM IMERG (sky blue). (**b**) The shade color represents 1000–300 hPa vertically integrated moisture condition and red streamline shows vertically integrated moisture flux at 18Z 27 August 2021.
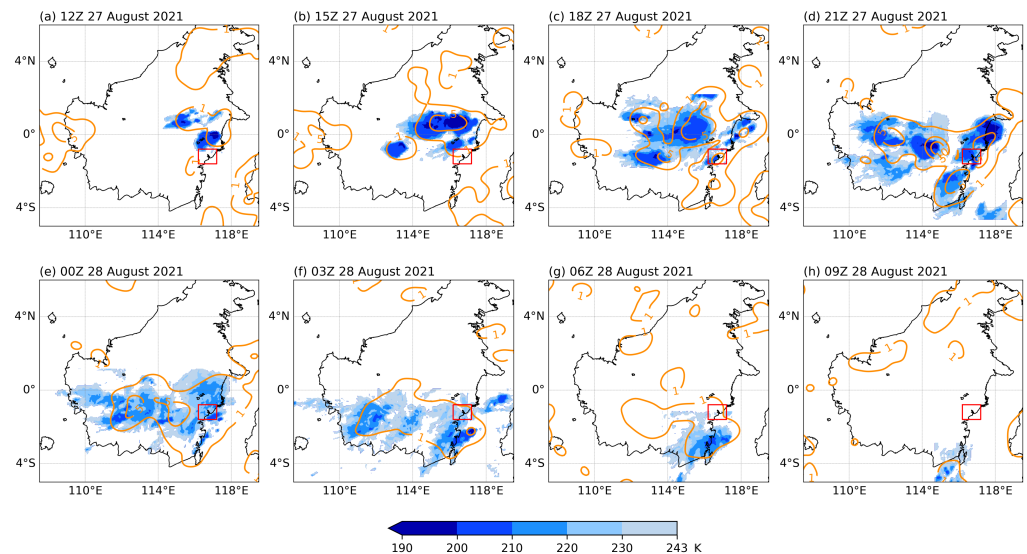
Figure 4. Three-hour evolution of the MCS (K, shaded) from Himawari-8 satellite superimposed with the rainfall rate from GPM IMERG (mm/h, contour) for the period of 27 August at 12Z to 28 August 2021 at 9Z. The location of Nusantara is denoted by a red box.

3.2.1. Dominant Moisture Origin, Pathways, and Contributions

Our results indicate that the higher moisture content (higher IVT) was detected over the Banda Sea and its surroundings (BSS), the South China Sea (SCS) and vicinity, and the Pacific Ocean near the equator (see Figure 3b). To accurately investigate the source and pathways of these moisture transports, the moisture over the flooding region was tracked back in time for 72 h before the peak rainfall on 27 August 2021 at 18Z (see Figure 5). To categorize these trajectories objectively, the pathways are grouped by *k*-mean clustering [39,40], resulting in three main clusters based on the elbow method [15,41]. The results show that the moisture responsible for the extreme rainfall event was transported from three directions: from the southeast as Cluster 1, from the northwest as Cluster 2, and from the east as Cluster 3 (see Figure 5b–d). Each cluster has distinct characteristics based on its moisture content. Specific humidity was higher over trajectories from the southeast in Cluster 1 (more than 12.5 g/kg) (see Figure 5b). The high specific humidity over this cluster was consistent with the more abundant moisture showed by the IVT magnitude over the Banda Sea and its vicinity (see Figure 3b). Moreover, the high specific humidity along the tracking was also detected from the northwest (Cluster 2), ranging from 7.5 g/kg to nearly 17.5 g/kg. The IVT vector explains that moisture is transported clockwise over the SCS and Borneo (see Figure 3b). Trajectories are consistent with IVT, which follows the anticyclonic flow over the SCS and then intrudes on Borneo to the flooding area (see Figure 5c). Some pathways in Cluster 2 also originated from the island of Borneo 72 h before heavy precipitation. These pathways from the SCS and the Borneo areas converged into the flooding area within Cluster 2 (see Figure 5c). Moreover, Cluster 3 has different moisture characteristics from the other clusters, with the fast westward movement of a drier air parcel (approximately less than 12.5 g/kg) (see Figure 5d). The velocity of the air parcel is shown by shorter pathways over 72 h. Overall, these moisture propagation regimes are consistent with the IVT vector, which illustrates the moisture transported toward the flooding location from various locations, including moisture movement from the southeast, east, and northwest (the IVT vector in Figure 3b). However, the result of the trajectories indicates more accurate pathways of moisture propagation toward Nusantara.
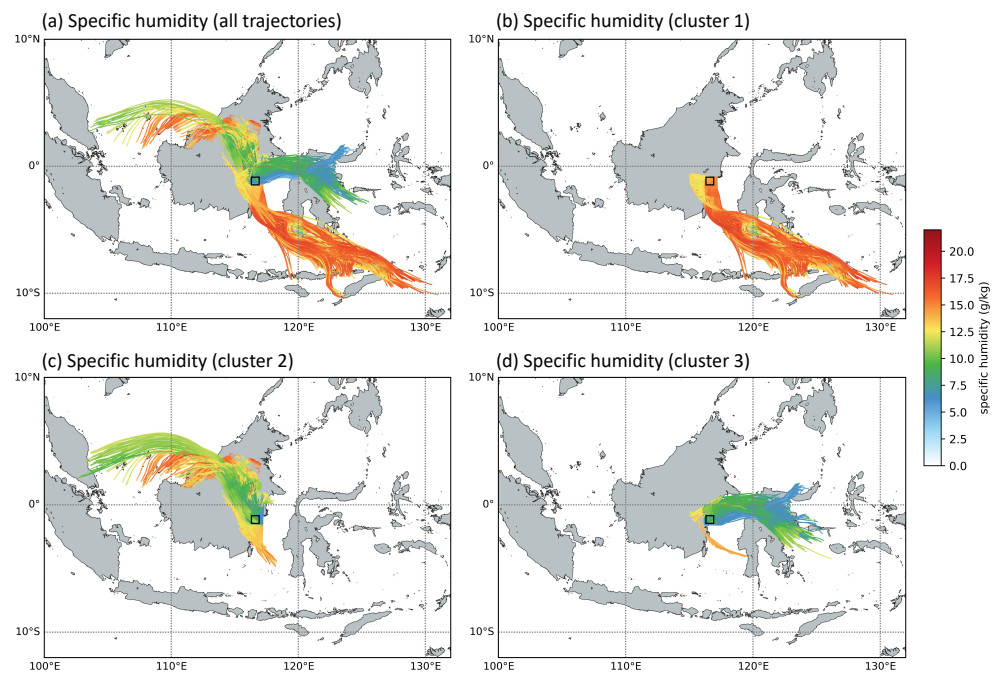
Figure 5. Seventy-two h backward trajectory of the moisture responsible for the extreme rainfall event over the Nusantara region (at 18Z, 27 Aug 2021). Trajectories (lines) and moisture concentration along the pathways (colors) for (**a**) all trajectories and (**b**) Cluster 1, (**c**) Cluster 2, and (**d**) Cluster 3.

The characteristics of moisture transport from each cluster are further explained by taking into account the vertical structure of trajectories. Figure 6 shows the altitude of the tracked air parcels within 72 h. The mean altitude of each cluster is calculated (solid line in Figure 6) and presented with its maximum and minimum value (shading in Figure 6). The results show that within Clusters 1–3, moisture arriving toward various release altitudes was dominated by moisture from the altitudes lower than 4.5 km. This is expected as the moist or humid air is found much below 5 km under a layer of warmer air in the lower troposphere [25].

Each cluster has a distinct characteristic based on its altitude profile. More specifically, Cluster 1 primarily advected horizontally from the southeast (Figure 5b) toward the study area over low altitudes (ranging from 0 to 1 km) (Figure 6). The low-level transport over this cluster denotes moisture exchange (moisture uptake and moisture outtake) over the earth's surface. Moreover, the additional moisture/moisture uptake over the lower altitude (planetary boundary layers) is closely related to the surface evaporation process [36]. Therefore, the indication of oceanic evaporation as the main mechanism of moisture uptake is strong as this cluster spreads along the BSS. In Section 3.2.2, we continue the discussion of the moisture transport drivers at the lower level toward Nusantara. Furthermore, Cluster 2 propagates horizontally from the northwest (Figure 5c) with an altitude between 0 and 2.1 km for 72–35 h prior to the extreme event. Within this cluster, the moisture ascended to an altitude between 1.8 and 2.8 km during t = 35–25 h prior to the peak of the extreme rainfall events. The ascending moisture can be reinforced by the interaction of shallow convection and low-level moisture convergence [43]. Moreover, the vertical wind shear magnitude is also one of the factors influencing updraft motion: the larger shear magnitude, the larger the moisture updraft [44]. Moreover, moisture that arrived from the east (from Sulawesi and its surroundings, Cluster 3) was mainly transported over higher altitudes (2.7 km on average) and converged over flooding locations at an altitude of 4.7 km. The fast propagation of air particles within Cluster 3 (shorter pathways in Figure 5d) can be explained by a higher wind speed in the free troposphere because there is no friction influenced by the roughness of the earth's surface. Furthermore, the additional moisture over the higher altitude was more likely through some mechanisms, such as convection and

evaporation of precipitating hydrometeors, or because of errors related to the numerical calculation of trajectories [36]. In more detail, the factors that drove the moisture transport from Clusters 2 and 3 toward Nusantara will be further discussed in Section 3.2.2.
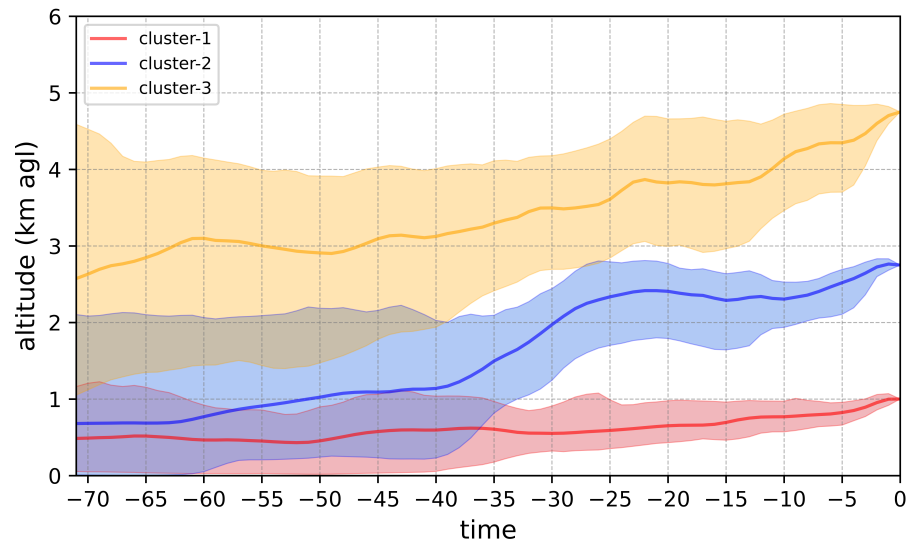

Figure 6. The evolution of moisture transport as a function of altitude and time prior to the extreme rainfall event (18Z, 27 August 2021) for each cluster. The solid line represents the mean altitude for each cluster, while the shading denotes the uncertainty of the moisture altitude.

Our results so far indicate that there are three main sources of moisture transport toward Nusantara, which produced the extreme rainfall event. To quantify the contribution of these moisture sources, we precisely calculated the integrated moisture intake over ten different regions and quantified its percentages (see Figure 7a–c). Similar to findings from previous studies (e.g., [36,37]), changes in moisture along the pathways can define the precipitation (moisture outtake) and evaporation (moisture intake) process along the pathways. We defined moisture intake as increasing moisture over time along its pathway ($\Delta q° > 0$), wherein the lower troposphere is highly correlated with evaporation (evaporative moisture uptake) [36]. Our results indicate that moisture intakes increase gradually over time, indicating the moistening of air parcels during their pathways upon arrival (see Figure 7b). The terrestrial moisture source is the dominant contributor to heavy rainfall, which accounts for 62.78% of the total moisture intake. Of the moisture, 53.73% evaporated over Borneo (BRN) and 9.05% over Sulawesi (SUL) (see Figure 7c). Moreover, the most significant oceanic moisture source, about 32.03%, is evaporated over BSS. About 3.77% of moisture intake is from the SCS, and 0.43% is from the Pacific Ocean and Surroundings (POS), making up the rest of the oceanic source of moisture for this heavy rainfall case (Figure 7c).
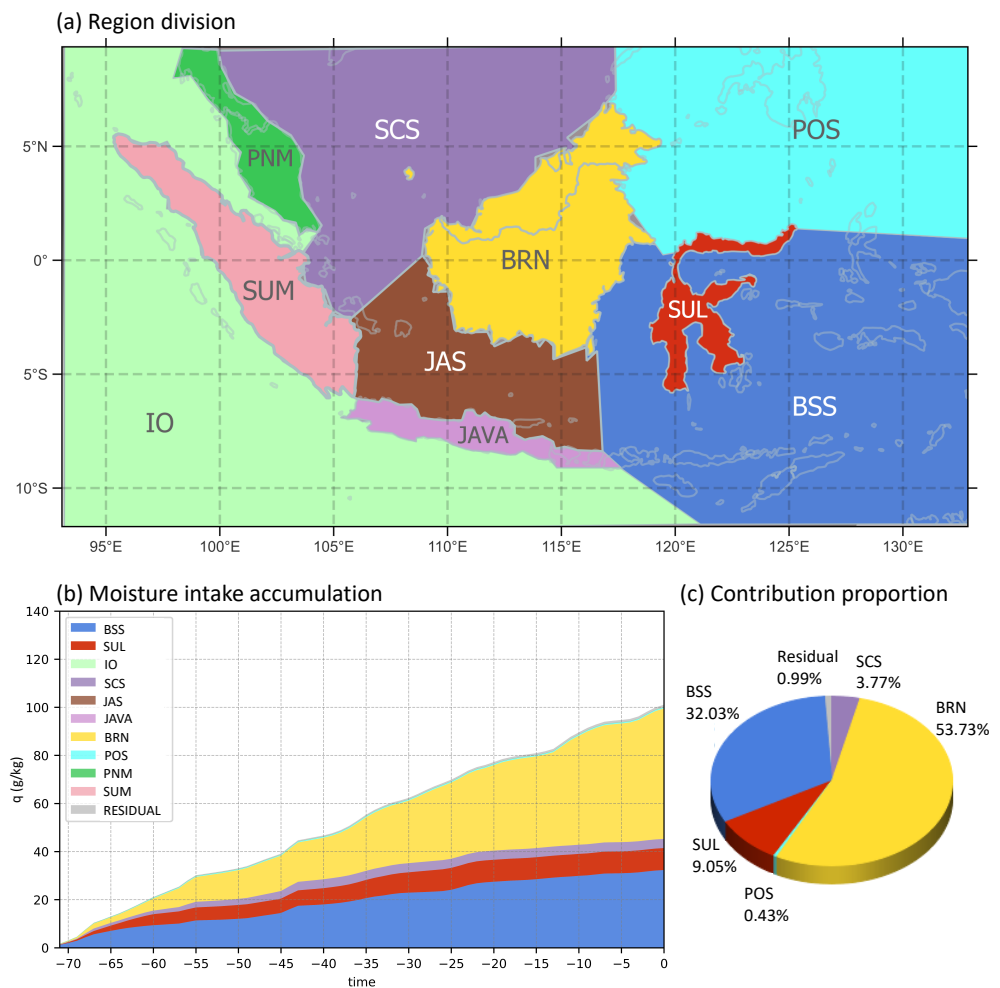
Figure 7. The moisture source contributions by different regions responsible for the extreme rainfal event. (**a**) The division of moisture source regions into 10 regions, including Peninsular Malaysia (PNM), Sumatera (SUM), Indian Ocean (IO), South China Sea (SCS), Java Sea (JAS), Java Island (JAVA), Borneo Island (BRN), Pacific Ocean and Surroundings (POS), Sulawesi Island (SUL), and Banda Sea and Surrounding (BSS). (**b**) The evolution of integrated moisture intake of the 10 sources along the trajectories in the target region. (**c**) The relative moisture contributions of different regions at the release time (0 days).

Further quantification of moisture contributions in each cluster from the different source regions is explained in Figure 8b,d,f, in which the moisture intake accumulation in a particular area helps to calculate this contribution, as shown in Figure 8a,c,e. Clearly, Cluster 1 is dominated by oceanic moisture sources from the BSS, which accounts for 92.3% of the total moisture intake over Cluster 1. The rest of the moisture sources are from terrestrial sources (BRN and SUL), where moisture is entrained to its pathways at a more stable pace. Moisture intake over the BSS location was detected for 72h before release and increased gradually until the release time. Sudden entrainment was detected over the BSS at 23–20 h before the heavy rainfall, indicating intensive evaporation over the ocean because this cluster was characterized by a moist air parcel with low-altitude moisture propagation (see Figures 5b and 6). As mentioned in the previous section, higher IVT was detected over BSS (see Figure 3b), and the specific humidity along this cluster's trajectories was higher than in the other clusters (see Figure 5b). Therefore, this cluster is essential as the moisture contributor to heavy precipitation. The Australian monsoon is suspected of atmospheric conditions corresponding to the pattern over this cluster, which is further explained in the following sub-section.
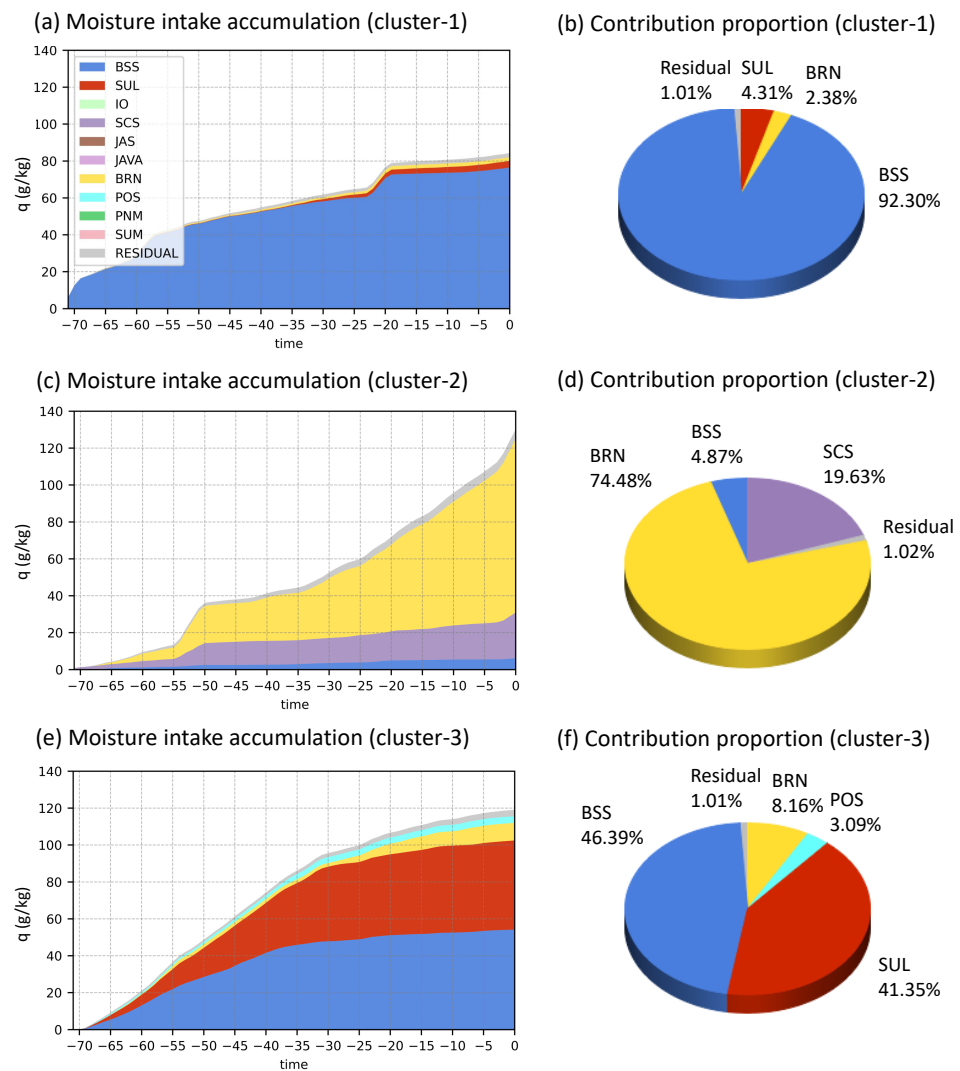
Figure 8. As in Figure 7b,c, but for the moisture intake in the three clusters.

In Cluster 2, approximately 74.48% of the moisture was transported from BRN with a relatively steep pattern, indicating faster moistening of the air parcel along the pathways over this area. It is worth noting that because the release point of the trajectory is also located over BRN as well, this cluster indicates moisture recycling. Moisture is recycled when the evaporation over an area contributes to the precipitation over the same area in which the evaporation is closely related to vegetation and a catchment area over the area [45,46]. This cluster was crucial to the moisture source of the extreme rainfall event in Nusantara because BRN accounts for half of the total moisture sources (see Figure 7), and the specific humidity along the trajectory is relatively high (see Figure 5c). This high relative humidity can also be explained by the MCS analysis indicating the intensive cloud formation, thus representing moisture intake over BRN (see Figure 4). Over this cluster, the SCS, as the oceanic moisture source, contributes 19.63% of the total moisture intake of this cluster. Furthermore, in Cluster 3, the contribution between terrestrial (SUL and BRN) and oceanic (BSS) moisture sources is comparable (Figure 8f). Terrestrial moisture sources contributed 49.51% of the moisture sources, and oceanic moisture sources contributed 46.39% of the moisture sources. The pattern shows that moisture intake increased at a nearly linear rate over this cluster (see Figure 8e).

In summary, our results indicate that the moisture responsible for the extreme rainfall in Nusantara on 27–28 August 2021 was mainly transported along three major routes:

from BRN, with a contribution of 53.73%; BSS, with a contribution of 32.03%; and SUL, with a contribution of 9.05%. In the following subsection, we explain the atmospheric conditions that drove the moisture transport within each cluster toward Nusantara.

3.2.2. The Role of Atmospheric Modes in the Variability of Moisture Transport

To understand the mechanisms responsible for driving the three main pathways of the moisture transport responsible for the extreme precipitation event in August 2021 in Nusantara, we deconstructed the IVT stream function during the event into different contributions of the atmospheric variability components. Figure 9 shows the decomposition of the total IVT stream function into the contribution of 10–20 days, 30–60 days, >120 days, and residual. The 10–20 day periodicity represents the contributions of high-frequency oscillation that are often associated with synoptic weather systems such as cyclones and anticyclones as well as the BSISO second mode (BSISO2) in the summer [47]. The 30–60 day periodicity is mainly associated with the BSISO first mode (BSISO1) in the summer [47]. The low-frequency variability (>120 days) is often associated with monsoonal flow, Indian Ocean Dipole (IOD), and ENSO [12,25,26,48]. Finally, the residual includes other contributions of other variability. In addition, we calculated the time series of climate indices associated with the Australian summer monsoon index (AUSMI), BSISO, Niño 3.4, and IOD to elucidate the drivers of such variability (see Figure 10).

Our results indicate that the near-surface moisture transport from the southwest (Cluster 1) toward Nusantara was mainly dominated by the low-frequency variability (>120 days) indicated by the dense stream function (see Figure 9a,d). We attribute this to the active phase of the Australian monsoon system (see Figure 10a). As seen in the time series of the AUSMI index, a strong and persistent Australian monsoon was observed with an amplitude ranging between −8 and −6 one week before the flood event (see Figure 10a). More importantly, this value increased from −7.2 m/s to −8.3 m/s on 27 and 28 August 2021. This indicates a strengthening of the near-surface southeasterly wind toward Nusantara. This strengthening is consistent with the warm SST over the Northern Hemisphere (Asia) and colder SST over the Southern Hemisphere (Australia) during boreal summer (not shown), which causes the wind to blow from high pressure in Australia to low pressure in Asia during the Australian monsoon [49]. An extensively warm SST in BSS enhanced the ocean evaporation that triggered intense moisture uptake throughout this circulation (not shown). Therefore, the prevailing wind pattern associated with the Australian monsoon system induced the near-surface southeasterly moisture transport from BSS to Nusantara (Cluster 1) as the most significant oceanic moisture origin.
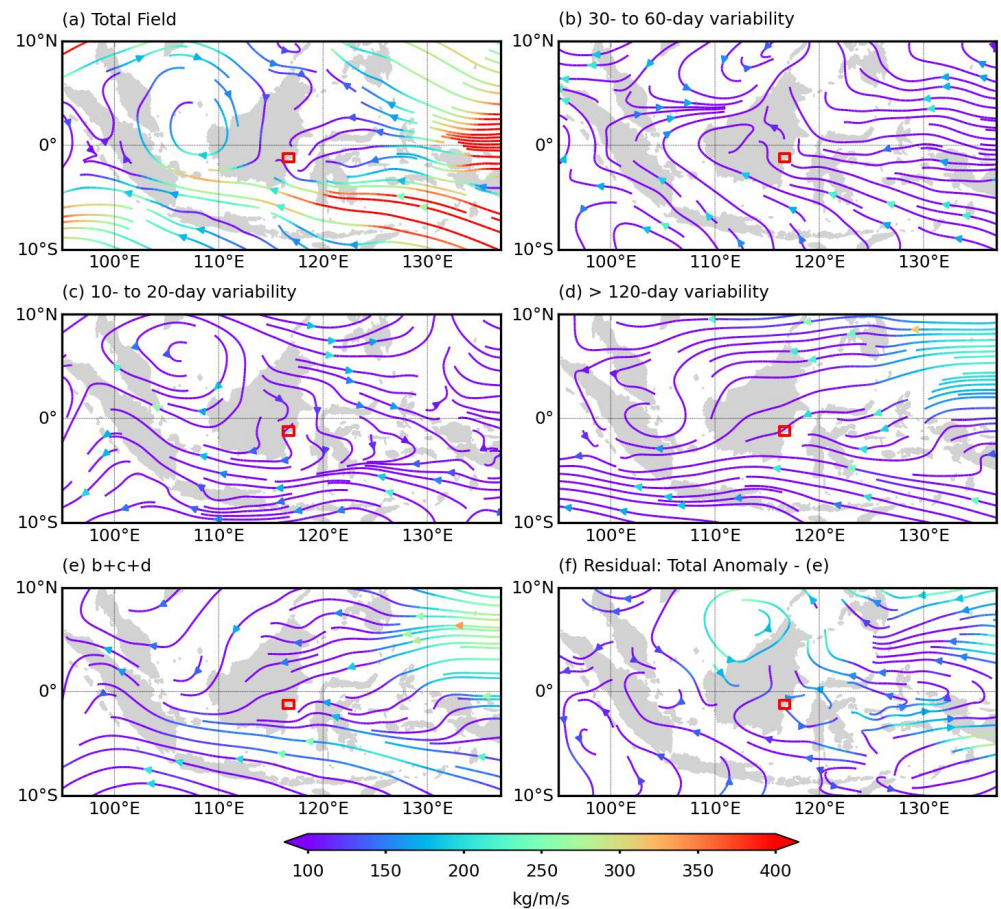
Figure 9. (**a**) The streamline of IVT during the period of extreme rainfall (27–28 August 2021) and its decomposition into contributions of (**b**) 30–60 day variability, (**c**) 10–20 day variability, (**d**) >120 day variability, (**e**) b + c + d, and (**f**) residual (total − (b + c + d). The streamlined colors denote the amplitude of IVT, and a red box denotes the location of Nusantara.

Furthermore, the activity of the high-frequency mode (10 to 20 days) associated with the large-scale high vortex flow located next to western BRN (see Figure 9c) was mainly explained by the transport from the SCS and BRN toward Nusantara. This circulation modulated the water vapor propagation from the SCS to BRN Island as the source of the oceanic moisture source in Cluster 2. Then, it initiated a favorable environment for the development of MCS that represents the moisture intake over BRN, contributing to the highest terrestrial moisture source for extreme precipitation events in Nusantara. However, boreal summer intraseasonal oscillation 2 (BSISO2), which is also identified as having 10-to-20-day variability, did not contribute to the enhanced moisture over Nusantara because it was in the weak amplitude of Phase 2 (see Figure 10b).

The westward transport of moisture toward Nusantara (Cluster 3) was mainly driven by the combined influence of 30-to-60-day and >120-day variability (see Figure 9b,d). The 30-to-60-day variability during summer is consistent with the active Phase 3 of BSISO1, where its amplitude exceeded the threshold value (more than 1, in Figure 10b). It then reached a peak of approximately 1.8 on 27–28 August 2021. This BSISO1-induced easterly circulation contributed to the moisture propagation from the eastern region of Indonesia toward Nusantara and its surrounding area (see Figure 10b). However, the low-frequency variability during this period is associated with La Niña, which also played an important role in this zonal transport (see Figure 10c). Those phenomena induced a relatively equal contribution of terrestrial (SUL and BRN) and oceanic (BSS) moisture sources over Cluster

3. The active La Niña strengthened the zonal circulation that modulates the propagation of moisture to Nusantara, resulting in extreme precipitation. Our findings further showed that low-frequency variability made a greater contribution than that of BSISO1 in modulating the easterly transport of moisture toward Nusantara (see Figure 9b,d).
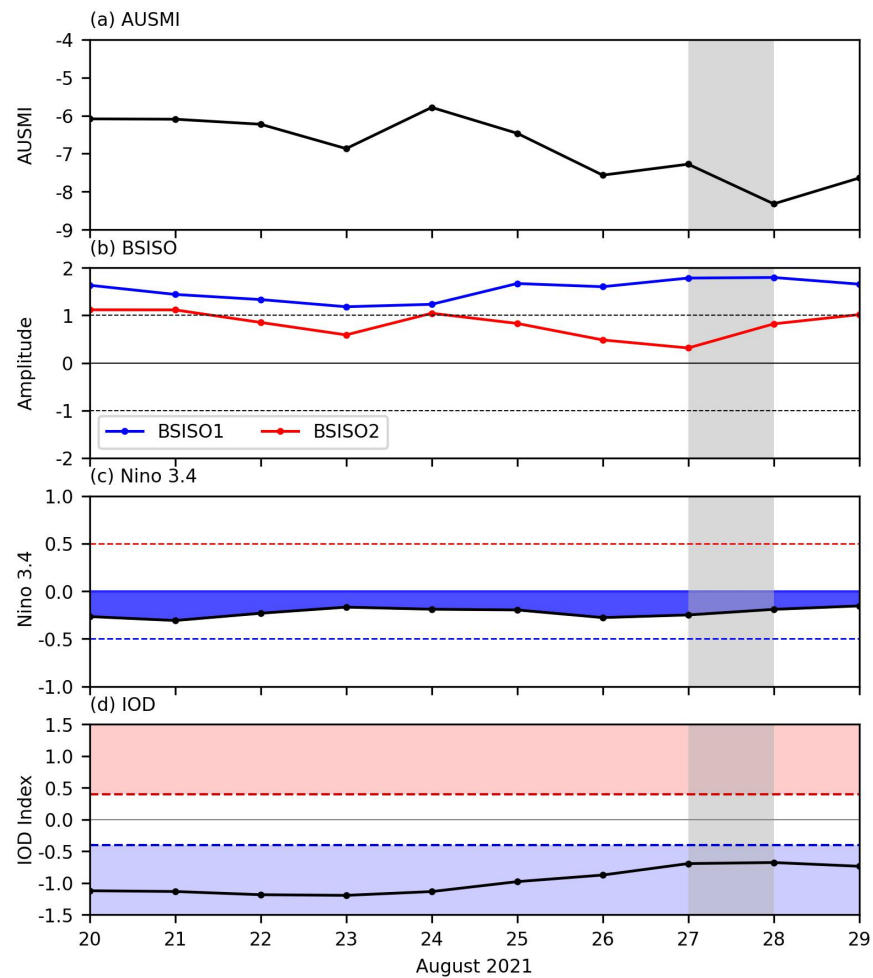

Figure 10. Daily time series of climate mode indices during 20–29 August 2021 for (**a**) AUSMI, (**b**) BSISO, (**c**) Nino 3.4, and (**d**) IOD. The grey color shows the flood event over Nusantara on 27–28 August 2021

In addition, we have examined a possible role of other variabilities, such as IOD (see Figure 10d). Our findings show that there was an active negative phase of IOD from 20 to 29 August 2021, with the threshold value of -1.0. A higher negative IOD index started on 20 August at about -1.2, then decreased gradually during the extreme precipitation event on 27–28 August to around -0.6. Even though IOD was in its active negative phase, which made it possible to drive the westerly zonal transport toward Nusantara, our results show that the streamline of low-frequency IVT was mainly dominated by the southeasterly and easterly transport associated with the Australian summer monsoon system and La-Niña circulations (see Figure 9), which suggest that IOD did not play an important role during this extreme event.

In summary, our results show that the transport of moisture from the southeasterly direction toward Nusantara (Cluster 1) was mainly driven by the low-frequency variability (>120 days) associated with the Australian summer monsoon system, whereas the north-westward transport of moisture (Cluster 2) was mainly driven by the anticyclonic activity having a synoptic periodicity of approximately 10–20 days. The combined influence of the

30-to-60-day oscillation associated with BSISO1 and the low-frequency variability associated with La Niña is responsible for driving the westward transport (Cluster 3) toward Nusantara during the extreme precipitation event.

4. Conclusions and Discussion

This study investigates the moisture transport and sources responsible for the extreme precipitation event over Indonesia's new capital city, Nusantara, on 27–28 August 2021, based on the HYSPLIT model using the ERA-5 reanalysis, satellite, and in situ data. Our major findings in this study are summarized as follows:

- The moisture responsible for the extreme precipitation event in Nusantara on 27–28 August 2021 was transported along three dominant routes: BRN, with a contribution of 53.73%; BSS, with a contribution of 32.03%; and SUL, with a contribution of 9.05%.
- BRN and SUL acted as the main sources of terrestrial moisture, whereas BSS acted as the main oceanic moisture source because most of the trajectories traveled across the ocean where the evaporation occurs.
- The Australian monsoon system significantly contributed to the oceanic moisture transport from BSS. A strong and persistent prevailing wind strengthened the near-surface flow passed through a warm sea-surface temperature in the BSS, which supported the large moisture intake from BSS.
- A large-scale high vortex flow located to the west of BRN contributed to the highest terrestrial moisture transport from BRN, whereas BSISO1 and low-frequency variability associated with La Niña modulated the moisture propagation from the eastern region of Indonesia.
- The results indicate the importance of terrestrial and oceanic moisture sources from BNN and SUL as well as BSS for the formation of extreme precipitation events in Nusantara, Indonesia.

The mechanisms driving the moisture transport during the extreme rainfall event in Nusantara are summarized in a schematic diagram in Figure 11. This diagram illustrates that the influence of the strong prevailing wind due to the Australian monsoon system was dominant at the near-surface layer to modulate the highest oceanic moisture source from the southeast region. Conversely, a large-scale high vortex circulation to the west of BRN transported the moist air from the SCS, favoring the development of MCS in BRN and contributing to the highest proportion of terrestrial moisture transport from BRN. Finally, the effects of BSISO1 and the low-frequency variability associated with La Niña play an important role in zonal circulation to supply the moisture from the eastern part of Indonesia and the Pacific Ocean to Nusantara.
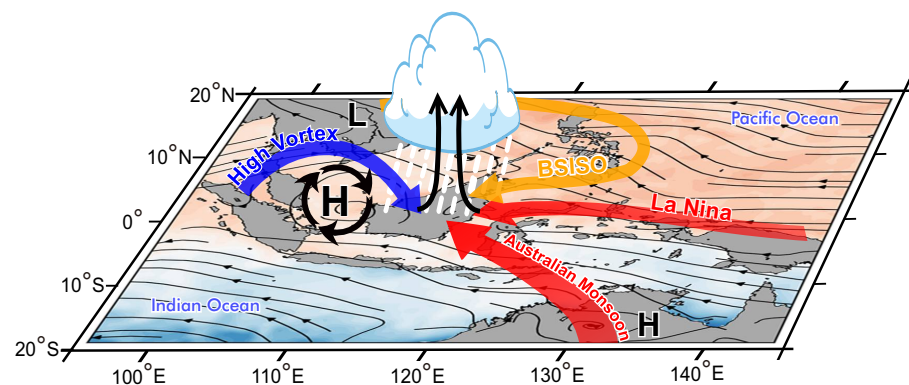

Figure 11. A conceptual diagram depicting the role of atmospheric modes in the variability of the moisture source regions during the flood event over Nusantara on 27–28 August 2021. Color shading denotes SST.

Previous studies have shown that the summer rainfall variability in East Kalimantan is influenced by several atmospheric modes, such as the Australian monsoon, ENSO, IOD, MJO, BSISO, and equatorial waves [8,50–55]. However, how the interaction among those atmospheric modes drove the extreme precipitation, which caused devastating flood events in east Kalimantan, from the perspective of moisture transport and sources, remains unknown. Our study is the first to show the mechanisms driving the extreme rainfall event in Indonesia through the lens of moisture transport and sources based on the Lagrangian approach while considering the underlying atmospheric drivers. Although our current study mostly focused on the large-scale transport of moisture responsible for the extreme rainfall event, other local forces, such as topography and land-sea breeze circulation, could create unique interactions that in turn drive moisture transport, resulting in extreme precipitation [53,56]. Therefore, understanding multiscale interactions among atmospheric phenomena resulting from extreme precipitation remains to be further studied.

The present study advances our understanding of the moisture sources and pathways for the extreme precipitation over Nusantara as well as the role of atmospheric modes in triggering moisture intake and propagation. These results can provide an important source of predictability for improving skilful prediction of extreme summer precipitation over Nusantara in the future, which, in turn, can be potentially used by multiple stakeholders in developing disaster management in Indonesia's new capital city, Nusantara.

Author Contributions: A.P., S.W.L., E.H., D.F.A., T.H., D.N.R., A.R., R. and A.P.S. are the main contributors. Conceptualization, S.W.L. and E.H.; methodology, S.W.L., A.P., R., A.R. and D.F.A.; software, A.R., A.P. and R.; validation, A.R.; formal analysis, S.W.L., A.P., R., A.R., E.H., T.H. and D.F.A.; Data, A.P., R., A.R., D.F.A., E.H. and T.H.; writing—original draft preparation, D.N.R., A.P., R., A.R. and D.F.A.; writing—review and editing, S.W.L. and D.N.R.; visualization, A.P., R., A.R. and D.F.A.; funding acquisition, E.H. All authors have read and agreed to the published version of the manuscript.

Institutional Review Board Statement: No applicable.

Informed Consent Statement: No applicable.

Data Availability Statement: The ERA-5 meteorological reanalysis dataset used in this study is available from the European Centre for Medium-Range Weather Forecasts (https://www.ecmwf.int/en/forecasts/datasets/reanalysis-datasets/era5, accessed on 30 March 2022). The hourly rainfall data from Global Precipitation Measurement (GPM) Integrated Multi-satellite Retrievals for GPM (IMERG) can be accessed freely through https://disc.gsfc.nasa.gov/datasets/ (accessed on 25 March 2022). The Himawari-8 satellite top brightness temperature (TBB) data and in situ hourly rainfall data presented in this study are available upon request from the corresponding authors.

Conflicts of Interest: The authors declare no conflict of interest.

References

1. Yusriyah, K.; Sudaryanto, S.; Fatoni, A.; Mansyur, M.A. Communication Networks Analysis on Information Dissemination of the Moving of Capital City From Jakarta to East Kalimantan. *Aspiration J.* **2020**, *1*, 31–55.
2. Nugroho, H. Pemindahan Ibu Kota Baru Negara Kesatuan Republik Indonesia ke Kalimantan Timur: Strategi Pemenuhan Kebutuhan dan Konsumsi Energi. *Bappenas Work. Pap.* **2020**, *3*, 33–41.
3. Kumalati, R.; Yuliarti, A.; Ali, S.D.; Murliawan, K.H.; Rahman, A.; Arief, O.E.A.; Muza, M.N.; Rinaldi, S.; Anggraini, R.N. Location Characteristics of the New Country Capital in East Kalimantan Province. *J. Antropol. Isu-Isu Sos. Budaya* **2022**, *24*, 18–25.
4. Abdul, M. Sebanyak 455 Rumah Terendam Banjir Kutai Kartanegara. Available online: https://www.bnpb.go.id/berita/-banjir-sebanyak-455-rumah-terendam-banjir-kutai-kartanegara- (accessed on 29 July 2022).
5. BMKG. Analisis Kejadian Banjir di Balikpapan Tanggal 28 Agustus 2021. Available online: https://www.bmkg.go.id/artikel/?p=analisis-kejadian-banjir-di-balikpapan-tanggal-28-agustus-2021&lang=ID (accessed on 30 July 2022).

6. Nurdiati, S.; Khatizah, E.; Najib, M.; Hidayah, R. Analysis of rainfall patterns in Kalimantan using fast fourier transform (FFT) and empirical orthogonal function (EOF). *J. Phys. Conf. Ser.* **2021**, *1796*, 012053.

7. Seo, K.H.; Schemm, J.K.E.; Wang, W.; Kumar, A. The boreal summer intraseasonal oscillation simulated in the NCEP Climate Forecast System: The effect of sea surface temperature. *Mon. Weather Rev.* **2007**, *135*, 1807–1827.

8. Muhammad, F.R.; Lubis, S.W.; Setiawan, S. Impacts of the Madden–Julian oscillation on precipitation extremes in Indonesia. *Int. J. Climatol.* **2021**, *41*, 1970–1984.

9. Jiang, X.; Li, T.; Wang, B. Structures and mechanisms of the northward propagating boreal summer intraseasonal oscillation. *J. Clim.* **2004**, *17*, 1022–1039.

10. Fukutomi, Y. Tropical Synoptic-Scale Waves Propagating Across the Maritime Continent and Northern Australia. *J. Geophys. Res. Atmos.* **2019**, *124*, 7665–7682.

11. Bjerknes, J. Atmospheric teleconnections from the equatorial Pacific. *Mon. Weather Rev.* **1969**, *97*, 163–172.

12. Aldrian, E.; Dwi Susanto, R. Identification of three dominant rainfall regions within Indonesia and their relationship to sea surface temperature. *Int. J. Climatol. A J. R. Meteorol. Soc.* **2003**, *23*, 1435–1452.

13. Aldrian, E. Spatial patterns of ENSO impact on Indonesian rainfall. *J. Sains Teknol. Modif. Cuaca* **2002**, *3*, 5–15.

14. Hassim, M.E.E.; Timbal, B. Observed Rainfall Trends over Singapore and the Maritime Continent from the Perspective of Regional-Scale Weather Regimes. *J. Appl. Meteorol. Climatol.* **2019**, *58*, 365–384. [CrossRef]

15. Córdova, M.; Orellana-Alvear, J.; Rollenbeck, R.; Célleri, R. Determination of Climatic Conditions Related to Precipitation Anomalies in the Tropical Andes by Means of the Random Forest Algorithm and Novel Climate Indices. *Int. J. Climatol.* **2021**, *42*, 5055–5072. [CrossRef]

16. Berry, G.; Reeder, M.J. Objective Identification of the Intertropical Convergence Zone: Climatology and Trends from the ERA-Interim. *J. Clim.* **2014**, *27*, 1894–1909. [CrossRef]

17. Freitas, A.C.V.; Aímola, L.; Ambrizzi, T.; de Oliveira, C.P. Extreme Intertropical Convergence Zone shifts over Southern Maritime Continent. *Atmos. Sci. Lett.* **2017**, *18*, 2–10. [CrossRef]

18. Mason, S.J.; Waylen, P.R.; Mimmack, G.M.; Rajaratnam, B.; Harrison, J.M. Changes in extreme rainfall events in South Africa. *Clim. Chang.* **1999**, *41*, 249–257. [CrossRef]

19. Westra, S.; Fowler, H.J.; Evans, J.P.; Alexander, L.V.; Berg, P.; Johnson, F.; Kendon, E.J.; Lenderink, G.; Roberts, N. Future changes to the intensity and frequency of short-duration extreme rainfall. *Rev. Geophys.* **2014**, *52*, 522–555.

20. Nie, Y.; Sun, J. Moisture Sources and Transport for Extreme Precipitation over Henan in July 2021. *Geophys. Res. Lett.* **2022**, *49*, e2021GL097446.

21. Zhou, Y.s.; Xie, Z.m.; Liu, X. An analysis of moisture sources of torrential rainfall events over Xinjiang, China. *J. Hydrometeorol.* **2019**, *20*, 2109–2122.

22. Tan, Y.; Yang, S.; Zwiers, F.; Wang, Z.; Sun, Q. Moisture budget analysis of extreme precipitation associated with different types of atmospheric rivers over western North America. *Clim. Dyn.* **2022**, *58*, 793–809.

23. Gimeno, L.; Dominguez, F.; Nieto, R.; Trigo, R.; Drumond, A.; Reason, C.J.; Taschetto, A.S.; Ramos, A.M.; RameshKumar, M.; Marengo, J. Major mechanisms of atmospheric moisture transport and their role in extreme precipitation events. *Annu. Rev. Environ. Resour.* **2016**, *41*, 117–141.

24. Gustafsson, M.; Rayner, D.; Chen, D. Extreme rainfall events in southern Sweden: Where does the moisture come from? *Tellus A: Dyn. Meteorol. Oceanogr.* **2010**, *62*, 605–616.

25. Hermawan, E.; Lubis, S.W.; Harjana, T.; Purwaningsih, A.; Ridho, A.; Andarini, D.F.; Ratri, D.N.; Widyaningsih, R. Large-Scale Meteorological Drivers of the Extreme Precipitation Event and Devastating Floods of Early-February 2021 in Semarang, Central Java, Indonesia. *Atmosphere* **2022**, *13*, 1092.

26. Lubis, S.W.; Hagos, S.; Hermawan, E.; Respati, M.R.; Ridho, A.; Muhammad, F.R.; Paski, J.A.I.; Ratri, D.N.; Setiawan, S.; Permana, D.S. Record-Breaking Precipitation in Indonesia's Capital Jakarta in January 2020 Linked to the Northerly Surge, Equatorial Waves, and MJO. *Earth Space Sci. Open Arch.* **2022**, 16. [CrossRef]

27. Hou, A.Y.; Kakar, R.K.; Neeck, S.; Azarbarzin, A.A.; Kummerow, C.D.; Kojima, M.; Oki, R.; Nakamura, K.; Iguchi, T. The Global Precipitation Measurement Mission. *Bull. Am. Meteorol. Soc.* **2014**, *95*, 701–722. [CrossRef]

28. Foelsche, U.; Kirchengast, G.; Fuchsberger, J.; Tan, J.; Petersen, W.A. Evaluation of GPM IMERG Early, Late, and Final rainfall estimates using WegenerNet gauge data in southeastern Austria. *Hydrol. Earth Syst. Sci.* **2017**, *21*, 6559–6572. [CrossRef]

29. Bessho, K.; Date, K.; Hayashi, M.; Ikeda, A.; Imai, T.; Inoue, H.; Kumagai, Y.; Miyakawa, T.; Murata, H.; Ohno, T.; et al. An Introduction to Himawari-8/9— Japan's New-Generation Geostationary Meteorological Satellites. *J. Meteorol. Soc. Jpn. Ser. II* **2016**, *94*, 151–183.

30. Putri, N.S.; Iwabuchi, H.; Hayasaka, T. Evolution of Mesoscale Convective System Properties as Derived from Himawari-8 High Resolution Data Analyses. *J. Meteorol. Soc. Jpn. Ser. II* **2018**, *96B*, 239–250.

31. Whitehall, K.; Mattmann, C.A.; Jenkins, G.; Rwebangira, M.; Demoz, B.; Waliser, D.; Kim, J.; Goodale, C.; Hart, A.; Ramirez, P.; et al. Exploring a graph theory based algorithm for automated identification and characterization of large mesoscale convective systems in satellite datasets. *Earth Sci. Inform.* **2015**, *8*, 663–675.

32. Nuryanto, D.E.; Pawitan, H.; Hidayat, R.; Aldrian, E. Characteristics of two mesoscale convective systems (MCSs) over the Greater Jakarta: Case of heavy rainfall period 15–18 January 2013. *Geosci. Lett.* **2019**, *6*, 1–15.

33. Hersbach, H.; Bell, B.; Berrisford, P.; Hirahara, S.; Horányi, A.; Muñoz-Sabater, J.; Nicolas, J.; Peubey, C.; Radu, R.; Schepers, D.; et al. The ERA5 global reanalysis. *Q. J. R. Meteorol. Soc.* **2020**, *146*, 1999–2049. [CrossRef]

34. Draxler, R.R.; Hess, G. An overview of the HYSPLIT_4 modelling system for trajectories. *Aust. Meteorol. Mag.* **1998**, *47*, 295–308.

35. Stein, A.F.; Draxler, R.R.; Rolph, G.D.; Stunder, B.J.B.; Cohen, M.D.; Ngan, F. NOAA's HYSPLIT Atmospheric Transport and Dispersion Modeling System. *Bull. Am. Meteorol. Soc.* **2015**, *96*, 2059–2077. [CrossRef]

36. Sodemann, H.; Schwierz, C.; Wernli, H. Interannual variability of Greenland winter precipitation sources: Lagrangian moisture diagnostic and North Atlantic Oscillation influence. *J. Geophys. Res. Atmos.* **2008**, *113*. [CrossRef]

37. Stohl, A.; James, P. A Lagrangian Analysis of the Atmospheric Branch of the Global Water Cycle. Part I: Method Description, Validation, and Demonstration for the August 2002 Flooding in Central Europe. *J. Hydrometeorol.* **2004**, *5*, 656–678. [CrossRef]

38. James, P.; Stohl, A.; Spichtinger, N.; Eckhardt, S.; Forster, C. Climatological aspects of the extreme European rainfall of August 2002 and a trajectory method for estimating the associated evaporative source regions. *Nat. Hazards Earth Syst. Sci.* **2004**, *4*, 733–746. [CrossRef]

39. Lou, D.; Yang, M.; Shi, D.; Wang, G.; Ullah, W.; Chai, Y.; Chen, Y. K-Means and C4.5 Decision Tree Based Prediction of Long-Term Precipitation Variability in the Poyang Lake Basin, China. *Atmosphere* **2021**, *12*, 834. [CrossRef]

40. Carvalho, M.; Melo-Gonçalves, P.; Teixeira, J.; Rocha, A. Regionalization of Europe based on a K-Means Cluster Analysis of the climate change of temperatures and precipitation. *Phys. Chem. Earth Parts A/B/C* **2016**, *94*, 22–28. [CrossRef]

41. Zhang, Y.; Moges, S.; Block, P. Optimal Cluster Analysis for Objective Regionalization of Seasonal Precipitation in Regions of High Spatial–Temporal Variability: Application to Western Ethiopia. *J. Clim.* **2016**, *29*, 3697–3717. [CrossRef]

42. Doblas-Reyes, F.J.; Déqué, M. A Flexible Bandpass Filter Design Procedure Applied to Midlatitude Intraseasonal Variability. *Mon. Weather Rev.* **1998**, *126*, 3326–3335. [CrossRef]

43. Liu, Y.; Tan, Z.M.; Wu, Z. Enhanced Feedback between Shallow Convection and Low-Level Moisture Convergence Leads to Improved Simulation of MJO Eastward Propagation. *J. Clim.* **2022**, *35*, 591–615. [CrossRef]

44. Peters, J.M.; Morrison, H.; Zhang, G.J.; Powell, S.W. Improving the Physical Basis for Updraft Dynamics in Deep Convection Parameterizations. *J. Adv. Model. Earth Syst.* **2021**, *13*, e2020MS002282. [CrossRef]

45. Trenberth, K.E. Atmospheric Moisture Recycling: Role of Advection and Local Evaporation. *J. Clim.* **1999**, *12*, 1368–1381. [CrossRef]

46. Savenije, H.H. New definitions for moisture recycling and the relationship with land-use changes in the Sahel. *J. Hydrol.* **1995**, *167*, 57–78. [CrossRef]

47. Muhammad, F.R.; Lubis, S. Impacts of the Boreal Summer Intraseasonal Oscillation (BSISO) on Precipitation Extremes in Indonesia. *Earth Space Sci. Open Arch.* **2022**, *35*. [CrossRef]

48. Supari.; Tangang, F.; Salimun, E.; Aldrian, E.; Sopaheluwakan, A.; Juneng, L. ENSO modulation of seasonal rainfall and extremes in Indonesia. *Clim. Dyn.* **2018**, *51*, 2559–2580. [CrossRef]

49. Wheeler, M.C.; McBride, J.L. Australian-Indonesian monsoon. In *Intraseasonal Variability in the Atmosphere-Ocean Climate System*; Springer: Berlin/Heidelberg, Germany, 2007; pp. 125–173.

50. Kurniadi, A. Pemilihan Ibukota Negara Republik Indonesia Baru Berdasarkan Tingkat Kebencanaan. *J. Manaj. Bencana (JMB)* **2019**, *5*, 3825–3839. [CrossRef]

51. As-syakur, A.R.; Adnyana, I.W.S.; Mahendra, M.S.; Arthana, I.W.; Merit, I.N.; Kasa, I.W.; Ekayanti, N.W.; Nuarsa, I.W.; Sunarta, I.N. Observation of spatial patterns on the rainfall response to ENSO and IOD over Indonesia using TRMM Multisatellite Precipitation Analysis (TMPA). *Int. J. Climatol.* **2014**, *34*, 3825–3839. [CrossRef]

52. Peatman, S.C.; Schwendike, J.; Birch, C.E.; Marsham, J.H.; Matthews, A.J.; Yang, G.Y. A local-to-large scale view of Maritime Continent rainfall: Control by ENSO, MJO and equatorial waves. *J. Clim.* **2021**, *34*, 8933–8953. [CrossRef]

53. Qian, J.H.; Robertson, A.W.; Moron, V. Diurnal cycle in different weather regimes and rainfall variability over Borneo associated with ENSO. *J. Clim.* **2013**, *26*, 1772–1790. [CrossRef]

54. Lubis, S.W.; Jacobi, C. The modulating influence of convectively coupled equatorial waves (CCEWs) on the variability of tropical precipitation. *Int. J. Climatol.* **2015**, *35*, 1465–1483. [CrossRef]

55. Lubis, S.W.; Respati, M.R. Impacts of convectively coupled equatorial waves on rainfall extremes in Java, Indonesia. *Int. J. Climatol.* **2021**, *41*, 2418–2440. [CrossRef]

56. Qian, J.H. Why precipitation is mostly concentrated over islands in the Maritime Continent. *J. Atmos. Sci.* **2008**, *65*, 1428–1441. [CrossRef]